

## Tuning Antiferromagnetism in DyFe<sub>2</sub>Al<sub>10</sub> via Ru Substitution

Koustav Pal\* and I.Das

Saha Institute of Nuclear Physics, A CI of Homi Bhabha National Institute, Kolkata 700064, India

**Citation:** Pal K, Das I. Tuning Antiferromagnetism in DyFe<sub>2</sub>Al<sub>10</sub> via Ru Substitution. *Int J Cur Res Sci Eng Tech* 2025; 8(2), 296-298. DOI: doi.org/10.30967/IJCRSET/Koustav-Pal/181

**Received:** 21 April, 2025; **Accepted:** 28 April, 2025; **Published:** 01 May, 2025

**\*Corresponding author:** Koustav Pal, Saha Institute of Nuclear Physics, A CI of Homi Bhabha National Institute, Kolkata 700064, India, E-mail: koustav.pal97@gmail.com

**Copyright:** © 2025 Pal K, et al., This is an open-access article distributed under the terms of the Creative Commons Attribution License, which permits unrestricted use, distribution, and reproduction in any medium, provided the original author and source are credited.

### ABSTRACT

We report the structural and magnetic properties of DyFe<sub>2</sub>Al<sub>10</sub> and its Ru-substituted counterpart DyFe<sub>1.75</sub>Ru<sub>0.25</sub>Al<sub>10</sub>. Rietveld refinement of X-ray diffraction data confirms that both compounds crystallize in the orthorhombic Cmc<sub>2</sub>m space group with high phase purity. Temperature-dependent magnetization measurements reveal antiferromagnetic ordering in both systems, with a Néel temperature of 7K for DyFe<sub>2</sub>Al<sub>10</sub> and 7.2K for the Ru-doped variant. A secondary magnetic anomaly near 25K is evident in DyFe<sub>1.75</sub>Ru<sub>0.25</sub>Al<sub>10</sub>, but absent in the parent compound. These results demonstrate the tunability of magnetic interactions in Dy-based aluminides via selective elemental substitution.

### Introduction

The diverse characteristics of electronic correlations continue to uncover novel aspects in condensed matter physics, particularly in magnetism, transport and theoretical frameworks. Intermetallic compounds with unique magnetic traits such as high coercivity, magnetization and giant magnetoresistance are crucial for applications in motors, generators and storage systems<sup>1-4</sup>. Rare-earth-based intermetallics are particularly noteworthy due to their large magnetic moments, complex magnetic structures and fascinating transport properties<sup>5-8</sup>. Among these materials, the family of RT<sub>2</sub>Al<sub>10</sub> (R = rare-earth, T = d-electron element) compounds has garnered significant attention. Initial studies focused on Ce derivatives, such as CeRu<sub>2</sub>Al<sub>10</sub>, CeFe<sub>2</sub>Al<sub>10</sub> and CeOs<sub>2</sub>Al<sub>10</sub>, due to their intriguing electronic behavior<sup>9-12</sup>. Within this series, CeRu<sub>2</sub>Al<sub>10</sub> and CeOs<sub>2</sub>Al<sub>10</sub> exhibit antiferromagnetic ordering with Néel temperatures (T<sub>N</sub>) of 27 K and 29 K, respectively, while CeFe<sub>2</sub>Al<sub>10</sub> behaves as a non-ordered Kondo insulator<sup>9,10,12</sup>.

In parallel, several studies have explored various rare earth-based compounds within this system, leading to the discovery of multiple magnetic phenomena, primarily driven by local

moments in heavy rare-earth compounds<sup>13-16</sup>. These materials crystallize in an orthorhombic structure, imparting substantial crystal electric field splitting energy, which influences their spin structures.

In compounds where T = Ru, such as RRu<sub>2</sub>Al<sub>10</sub> (R = Nd, Gd) and ROs<sub>2</sub>Al<sub>10</sub> (R = Nd, Sm, Gd), antiferromagnetic phase transitions occur<sup>13-15</sup>. However, compounds like RRu<sub>2</sub>Al<sub>10</sub> (R = La, Pr, Yb) and ROs<sub>2</sub>Al<sub>10</sub> (R = La, Pr) show non-magnetic behavior<sup>15,16</sup>. In the case of T = Fe, magnetic measurements reveal that RFe<sub>2</sub>Al<sub>10</sub> (R = Sm, Gd, Tb, Dy, Er, Tm) exhibit antiferromagnetism, while compounds like RFe<sub>2</sub>Al<sub>10</sub> (R = Y, La, Pr, Ho, Yb) show no magnetic ordering<sup>17-21</sup>. The ferromagnetic quantum criticality observed in YFe<sub>2</sub>Al<sub>10</sub> and YbFe<sub>2</sub>Al<sub>10</sub> is linked to the unique nature of Fe's electronic interactions<sup>22</sup>.

DyFe<sub>2</sub>Al<sub>10</sub>, in particular, exhibits an intriguing helical antiferromagnetic structure at T<sub>N</sub> = 7.5 K<sup>20</sup>. Despite these advances, there remains a significant gap in understanding the electrical transport properties and their interplay with magnetism, especially in the context of magneto-transport. To address this, our study focuses on DyFe<sub>2</sub>Al<sub>10</sub>, exploring its magnetic and transport properties, while also investigating

the impact of Ru substitution. This work aims to deepen our understanding of these materials and stimulates further research into their potential applications, particularly in the realm of giant magnetoresistance.

## Experimental Details

Polycrystalline samples of  $\text{DyFe}_2\text{Al}_{10}$  and  $\text{DyFe}_{1.75}\text{Ru}_{0.25}\text{Al}_{10}$  were synthesized using an arc melting technique. High-purity elements-Dy, Fe, Ru and Al (each with a purity greater than 99.99%)-were weighed in stoichiometric proportions and repeatedly arc-melted under a high-purity argon atmosphere to ensure homogeneity. The resulting ingots were then sealed in evacuated quartz tubes and annealed at 850 °C for 7 days to promote crystallinity and phase uniformity<sup>23</sup>.

Room-temperature X-ray diffraction (XRD) patterns were recorded using a Rigaku diffractometer equipped with Cu-K $\alpha$  radiation<sup>24</sup>. Structural analysis was conducted via Rietveld refinement using the Full Prof Suite to confirm phase formation and determine the lattice parameters.

Magnetic measurements were performed using a Superconducting Quantum Interference Device (SQUID) magnetometer and a Physical Property Measurement System (PPMS). Approximately 20mg of each sample was used for SQUID measurements. The SQUID system operates in the 2-400K temperature range and under magnetic fields up to 7T<sup>25</sup>. Complementary measurements were conducted using the PPMS, which offers similar capabilities with a magnetic field limit of 9 T<sup>26</sup>.

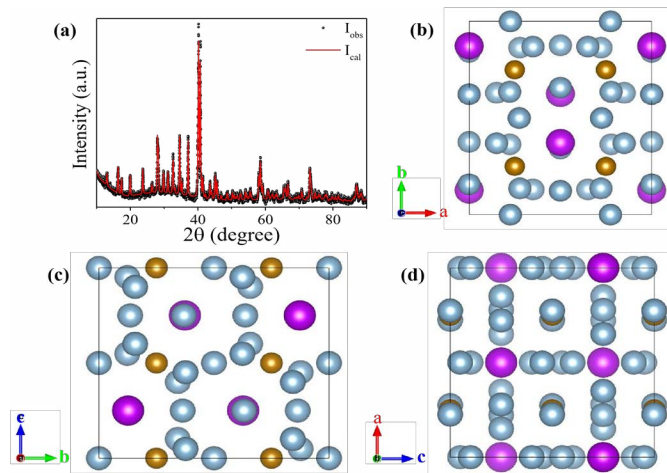


**Figure 1:** (a) Full Rietveld refinement of the room-temperature (300K) X-ray diffraction (XRD) pattern of the powdered polycrystalline  $\text{DyFe}_2\text{Al}_{10}$  compound. (b–d) Three-dimensional representations of the crystal structure along different crystallographic orientations. Dysprosium (Dy), iron (Fe) and aluminum (Al) atoms are depicted in magenta, brown and gray, respectively.

## Results and Discussion

### Structural properties

Figure 1(a) presents the room-temperature XRD pattern of  $\text{DyFe}_2\text{Al}_{10}$  along with the corresponding Rietveld refinement fit. The results confirm that the compound crystallizes in the orthorhombic  $\text{Cmcm}$  space group. The absence of secondary phases within the instrument's resolution attests to the high phase purity of the sample. The refined lattice parameters are  $a = 8.95(4)$  Å,  $b = 10.15(4)$  Å and  $c = 9.00(4)$  Å. Figures 1(b–d)

illustrate the unit cell of  $\text{DyFe}_2\text{Al}_{10}$ , where Dy, Fe and Al atoms are represented in magenta, brown and gray, respectively.

### Magnetic properties

To investigate magnetic interactions, temperature dependent magnetization measurements,  $M(T)$ , were performed under various magnetic field strengths using zero-field-cooled (ZFC), field-cooled cooling (FCC) and field-cooled warming (FCW) protocols over a temperature range of 3-380K.

Figures 2(a-b) show the  $M(T)$  curves recorded at 100Oe for  $\text{DyFe}_2\text{Al}_{10}$  and  $\text{DyFe}_{1.75}\text{Ru}_{0.25}\text{Al}_{10}$ , respectively. The inset of Figure 2(b) highlights the near overlap of the FCC and FCW curves, indicating no structural phase transition during thermal cycling.

The Néel temperature ( $T_N$ ) of  $\text{DyFe}_2\text{Al}_{10}$  is approximately 7K, while that of  $\text{DyFe}_{1.75}\text{Ru}_{0.25}\text{Al}_{10}$  is slightly elevated to 7.2K, suggesting that Ru substitution enhances magnetic ordering. Moreover,  $\text{DyFe}_{1.75}\text{Ru}_{0.25}\text{Al}_{10}$  exhibits a low-temperature bifurcation near 25K in its magnetization curves, a feature not observed in the parent compound, indicating possible.

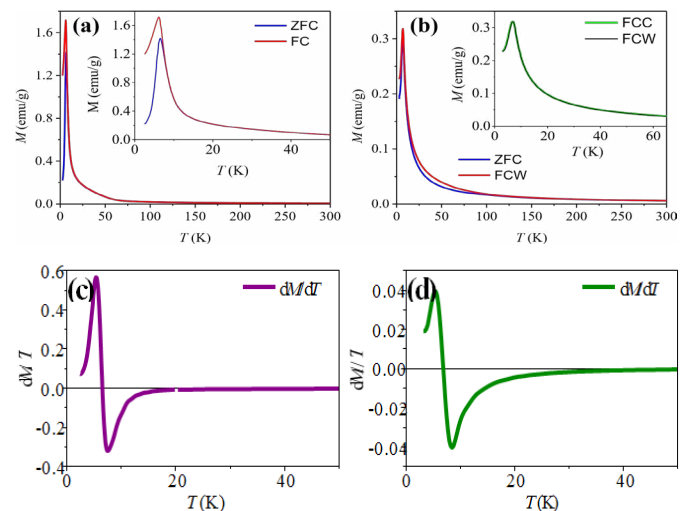


**Figure 2:** (a) Temperature-dependent magnetization,  $M(T)$ , measured under zero-field-cooled (ZFC) and field-cooled (FC) protocols at an applied magnetic field of 100Oe for  $\text{DyFe}_2\text{Al}_{10}$ . The inset shows a magnified view of the  $M(T)$  curve. (b)  $M(T)$  measured under ZFC and FC protocols at 100Oe for  $\text{DyFe}_{1.75}\text{Ru}_{0.25}\text{Al}_{10}$ . The inset highlights the near-perfect overlap between the FCC and FCW curves, indicating thermal reversibility. (c) and (d) Derivative plots,  $dM/dT$ , for  $\text{DyFe}_2\text{Al}_{10}$  and  $\text{DyFe}_{1.75}\text{Ru}_{0.25}\text{Al}_{10}$ , respectively.

spin reorientation or secondary magnetic interactions induced by Ru incorporation. Figures 2(c) and 2(d), which present the derivative plots  $dM/dT$ , further corroborate this suppression. While a pronounced anomaly is visible around 25K in  $\text{DyFe}_2\text{Al}_{10}$ , a much smoother response is observed in  $\text{DyFe}_{1.75}\text{Ru}_{0.25}\text{Al}_{10}$ , implying the stabilization of the antiferromagnetic ground state upon Ru doping.

### Discussion

The structural analysis of  $\text{DyFe}_2\text{Al}_{10}$  confirms that it crystallizes in the orthorhombic  $\text{Cmcm}$  space group, with no secondary phases detected, indicating high phase purity. The lattice parameters obtained from Rietveld refinement are  $a = 8.95(4)$  Å,  $b = 10.15(4)$  Å and  $c = 9.00(4)$  Å. Magnetization measurements reveal that both  $\text{DyFe}_2\text{Al}_{10}$  and  $\text{DyFe}_{1.75}\text{Ru}_{0.25}\text{Al}_{10}$

exhibit antiferromagnetic ordering with a Néel temperature ( $T_N$ ) of 7K and 7.2K, respectively, suggesting that Ru substitution enhances magnetic ordering. Notably,  $\text{DyFe}_{1.75}\text{Ru}_{0.25}\text{Al}_{10}$  exhibits a bifurcation near 25K in its magnetization curve, which is absent in the parent compound, indicating potential spin reorientation or secondary magnetic interactions induced by Ru doping. The derivative plots  $dM/dT$  further support this, showing a pronounced anomaly around 25K in  $\text{DyFe}_2\text{Al}_{10}$ , while  $\text{DyFe}_{1.75}\text{Ru}_{0.25}\text{Al}_{10}$  displays a smoother response, implying the stabilization of the antiferromagnetic ground state upon Ru doping. These results highlight the tunability of magnetic interactions in  $\text{DyFe}_2\text{Al}_{10}$  via Ru substitution, offering insights into the modification of its magnetic properties.

## Conclusion

The structural and magnetic properties of  $\text{DyFe}_2\text{Al}_{10}$  and  $\text{DyFe}_{1.75}\text{Ru}_{0.25}\text{Al}_{10}$  reveal that Ru substitution enhances magnetic ordering, as evidenced by the slight increase in the Néel temperature and the appearance of a low-temperature bifurcation in the magnetization curves of the Ru-doped compound. The smooth  $dM/dT$  response in  $\text{DyFe}_{1.75}\text{Ru}_{0.25}\text{Al}_{10}$  suggests stabilization of the antiferromagnetic ground state upon Ru doping. These findings emphasize the potential of Ru substitution to modulate magnetic interactions in  $\text{DyFe}_2\text{Al}_{10}$ , providing valuable insights into the tuning of its magnetic properties.

## Acknowledgments

This work was supported by the Department of Atomic Energy (DAE), Government of India.

## Data Availability Statement

The data that support the findings of this study are available from the corresponding author upon reasonable request.

## References

1. Barna's J and Dugaev VK. Handbook of Surface Science 2015;5:371.
2. Wu H, Chen A, Zhang P, et al. Magnetic memory driven by topological insulators. Nature communications 2021;12:6251.
3. Pal K and Das I. Exploring the exchange bias of Gd and MnPt: A combined structural and magnetic investigation. Thin Solid Films 2024;790:140211.
4. Pal K, Dey S, Alam A and Das I. Revealing exchange bias in spin compensated systems for spintronics applications. Scientific Reports 2024;14:30678.
5. Shao Z and Ren S. Rare-earth-free magnetically hard ferrous materials. Nanoscale Advances 2020;2:4341.
6. Wang X, Tang Y, Lee J-M and Fu G. Rare-Earth Single-Atom Catalysts: A New Frontier in Photo/Electrocatalysis. Chem Catalysis 2022.
7. Liang S, Wang H, Li Y, et al. Rare-earth based nanomaterials and their composites as electrode materials for high performance supercapacitors: a review. Sustainable Energy Fuels 2020;4:3825.
8. Pal K, Dey S and Das I. J Physics: Condensed Matter 2024;36:215802.
9. Strydom AM. A review of the Kondo insulator materials class of strongly correlated electron systems: Selected systems and anomalous Behavior. Physica B: Condensed Matter 2009;404:2981.
10. Khalyavin D, Hillier A, Adroja D, et al, et al. Physical Review 2010;82:100405.
11. Nishioka T, Hirai D, Kawamura Y, et al. J Physics: Conference Series 2011;273:012046.
12. Kato H, Takesaka T, Kobayashi R, et al. A NQR Study of  $\text{CeOs}_2\text{Al}_{10}$ . J Physics: Conference Series 2011;273.
13. Tanida H, Tanaka D, Sera M, et al, et al. Physical Review B 2011;84:115128.
14. Sera M, Nohara H, Nakamura M, Tanida H, Nishioka T and Matsumura M. Physical Review B 2013;88:100404.
15. Morrison G, Haldooarachchige N, Young DP and Chan JY. J Physics: Condensed Matter 2012;24:356002.
16. Muro Y, Kajino J, Onimaru T and Takabatake T. J Physical Society of Japan 2011;80:021.
17. Reehuis M, Wolff M, Krimmel A, et al. J Physics: Condensed Matter 2003;15:1773.
18. Strydom A and Peratheepan P. physica status solidi (RRL)-Rapid Research Letters 2010;4:356.
19. Strydom AM, Peratheepan P, Sarkar R, Baenitz M and Steglich F. J Physical Society of Japan 2011;80:043.
20. Reehuis M, Fehrmann B, Wolff M, Jeitschko W and Hofmann M. Physica B: Condensed Matter 2000;276:594.
21. Sera M, Nohara H, Nakamura M, Tanida H, Nishioka T and Matsumura M. Physical Review B 88:100404
22. (2013).
23. Khuntia P, Strydom A, Wu L, Aronson M, Steglich F and Baenitz M. Physical Review B 2012;86:220401.
24. Pal K, Dey S and Das I. J Materials Chem C 2024;12:14936.
25. Pal K and Das I. Journal of Alloys and Compounds 2023;960:170794.
26. Pal K and Das I. Applied Materials Today 2024;39:102316.
27. Pal K, Mandal S and Das I. Acta Materialia 2024;278:120276.